


Research Article

Investigation of High-Temperature Wear Behaviour of AA 2618-Nano Si₃N₄ Composites Using Statistical Techniques

Santhi M. George,¹ Amel Gacem,² A. Kistan,³ R. Mohammed Ashick,⁴ L. Malleswara Rao,⁵ Vinod Singh Rajput,⁶ N. Nagabooshanam,⁷ Moamen S. Refat,⁸ Annah Mohammed Alsuhaibani,⁹ and David Christopher ¹⁰

¹Department of Science and Humanities, RMK Engineering College, Thiruvallur, Tamil Nadu 601206, India

²Department of Physics, Faculty of Sciences, University 20 Août 1955, 26 El Hadaiek, Skikda 21000, Algeria

³Department of Chemistry, Panimalar Engineering College, Chennai, Tamil Nadu 600123, India

⁴Department of Civil Engineering, Sri Sairam Engineering College, Chennai, Tamil Nadu 600044, India

⁵Department of Physics, SRI Y N College, Narsapur, West Godavari, Andhra Pradesh 534275, India

⁶Department of Mechanical Engineering, Nowgong Engineering College, Nowgong, Chhatarpur, Madhya Pradesh 471201, India

⁷Department of Mechanical Engineering, Aditya Engineering College, ABD Road, Surampalem, 533437 Andhra Pradesh, India

⁸Department of Chemistry, College of Science, Taif University, P.O. Box 11099, Taif 21944, Saudi Arabia

⁹Department of Physical Sport Science, College of Education, Princess Nourah bint Abdulrahman University, P.O. Box 84428, Riyadh 11671, Saudi Arabia

¹⁰Department of Mechanical Engineering, College of Engineering, Wolaita Sodo University, Ethiopia

Correspondence should be addressed to David Christopher; david.santosh@wsu.edu.et

Received 8 May 2022; Revised 17 July 2022; Accepted 18 July 2022; Published 16 September 2022

Academic Editor: Arpita Roy

Copyright © 2022 Santhi M. George et al. This is an open access article distributed under the Creative Commons Attribution License, which permits unrestricted use, distribution, and reproduction in any medium, provided the original work is properly cited.

The wear behaviour of hot pressed AA 2618 aluminium alloy matrix composites reinforced through nano Si₃N₄ elements (1 percent and 2 percent) has been investigated in this paper. Temperatures of 50°C, 150°C, and 250°C were used to examine the tribological characteristics of the models under a range of loads and pressures. The best wear performance was found in AA 2618/2wt percent Si₃N₄. Under a load of 30 N and temperature of 250°C, it was discovered that Si₃N₄-enriched AA 2618 alloy was 35.7% more wear-resistant than unreinforced AA 2618 alloy. Metal flow and plain delamination were the most common wear mechanisms at higher temperatures. Delamination is the most common wear mechanism at temperatures between 50 and 250 degrees Celsius. In the analysis of variance, the wear rate was influenced by temperature, load, and the presence of Si₃N₄ by 47.2%. In order to predict the wear rate, regression equations (linear and nonlinear) were developed by Taguchi method. Using a high determination coefficient, the nonlinear regression was the preeminent success rate (92.8 percent).

1. Introduction

Lightweight, inexpensive, and energy-efficient alloys are becoming increasingly popular. It is broadly used in the automotive industries for its maximum specific strength, corrosion resistance, and excellent low-temperature properties [1]. Although Al alloys have some drawbacks, the most significant one is their less amount of wear and mechanical properties at higher temperatures [2, 3]. Al metal matrix

composites have been developed to address these shortcomings (AMMCs). Al MMCs are commonly reinforced with a variety of materials, including SiC, Al₂O₃, B₄C, TiC, CNT, GNPs, GO, and Y₂O₃ [4]. Since Si₃N₄ has a high melting point and good thermal conductivity, it was a natural choice for Al MMC reinforcement. Research into MMCs' wear and friction patterns is essential [5–7]. In the event that two surfaces are in close proximity to each other, material loss can occur. Consequently, wear has become a major cause of

failure. MMCs wear more quickly when subjected to varying loads, sliding speeds, temperatures, and reinforcement content [8, 9]. Statistics and the Taguchi method have become increasingly popular in the field of materials science in recent years. The Taguchi method reduces the amount of time and money required to conduct experiments in order to optimise design parameters [10]. Wear rates and friction coefficients can be studied using the analysis of variance method. Wear rate is also predicted using a regression model. The wear behaviour of AA 2618 matrix composites has been studied by researchers. In addition to silicon carbide, aluminium oxide, and carbon nanotubes, a variety of reinforcements were used [11, 12]. While some research has been done on the tribological performance of stir cast AA 2618/Si₃N₄ composite (wt% of 3, 6, and 9 Si₃N₄ content), only a few studies have focused on the properties of 6 percent Si₃N₄. AA 2618/Si₃N₄ (4 wt%) composites were stir casted to investigate the dry sliding wear behaviour [13]. They found that composites have a higher wear resistance than AA 2618 alloy without reinforcement. It has dry sliding tribological properties at elevated temperatures between 30 and 300 degrees Celsius. The fabricated MMCs by stir casting were attributed to the increase in wear resistance [14–16]. The wear performance of AA 2618-SiC-hSi₃N₄ nanocomposites has been improved by the addition of SiC and hSi₃N₄ particles [17–20]. There have been numerous studies on AA 2618/Si₃N₄ composites based on the literature. A liquid metallurgy production method was used in these studies [21]. Additionally, statistical analysis was not used to examine the wear behaviour of the samples. Furthermore, no research has been done on the wear behaviour of monolithic AA 2618/Si₃N₄ composites made by powder metallurgy at elevated temperatures [22–26]. Fuselage structures below tension frequently use AA 2618 alloy because of its high specific strength, good machinability, and high fatigue strength and thermal conductivity [27]. The AA 2618 alloy's tribological performance is known to be poor at high temperatures. Ceramic particles have been added to AA 2618 alloy in order to increase its usefulness in high-temperature applications [28–30]. It is revealed that AA 2618 wear behaviour at elevated temperatures must be studied and improved. An investigation into hot pressing AA 2618/Si₃N₄ composites armoured with Si₃N₄ (1% wt and 2% wt) was primary goal of this research [31]. Different parameters (such as load, Si₃N₄ content, and temperature) were examined for their effects on wear rate using analysis of variance and regression models. It was also used in the search for the best process parameter that had the lowest wear rate [32–34].

2. Experimental Studies

2.1. Production and Materials. AA 2618 alloy powder was used as a matrix material in this research. Because of its ability to work at higher temperatures, AA 2618 is frequently used as pistons and spinning aviation components, as well as in automotive racing. The AA 2618 alloy chemical composition was determined to be 4.7Cu, 1.6Mg, 0.6Zn, 0.5Mn, and 0.2Si and a weight percentage of Al that was bal-

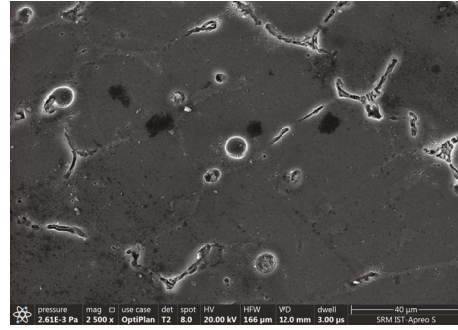


FIGURE 1: SEM image of powder used.

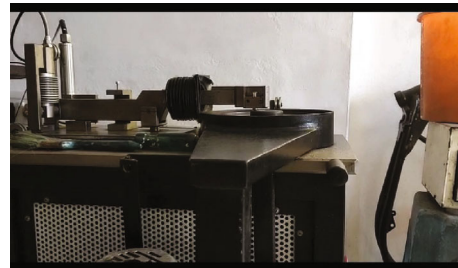


FIGURE 2: Pin on disc wear setup.

TABLE 1: Test parameters for measuring wear.

Levels	Applied load, N	Temperature °C	Wt percent of silicon nitrate
1	15	50	0
2	30	150	1
3	45	250	2

anced. Reinforcement was provided by Si₃N₄ nanoparticles (100 nm). The composites were made using semi-powder metallurgy. To separate the agglomerated particles, Si₃N₄ particles were ultrasonically treated in ethanol for one hour. Next, AA 2618 alloy powder was added to the solution containing Si₃N₄ nanoparticles. In a vacuum distillation system, a magnetic stirrer was used to mix the powders (AA 2618 alloy and Si₃N₄). After three hours, all of the ethanol had been flushed from the system. Previous studies provided a schematic diagram and detailed explanation of semi-powder metallurgy. Si₃N₄ nanoparticles of 0, 1, and 2wt percent were used in the samples. One hour of hot pressing at 525°C under 50 MPa pressure produced the test specimens. The rate of heating was 10°C/min. In an argon atmosphere, all the processes were carried out. Due to the size requirements of this study, the attained samples of 15 mm x 23 mm were maintained. Figure 1 shows SEM image of powder used.

2.2. Mechanical and Wear Tests. A hardness test device was used to take the hardness measurements. It was necessary to

TABLE 2: Specimens' densities and hardness.

Materials	(density) _{theoretical} g/cm ³	(density) _{Experimental} g/cm ³	(density) _{Relative} g/cm ³	Hardness, HV	% of raise in hardness
AA 2618	3.71	3.76	97.1	81.4 ± 3.6	92.4 ± 1.6
AA 2618/1% silicon nitrate	3.82	3.780	98.4	98.1	94.8 ± 1.9
AA 2618/2% silicon nitrate	3.78	3.798	9.4	16.2	10

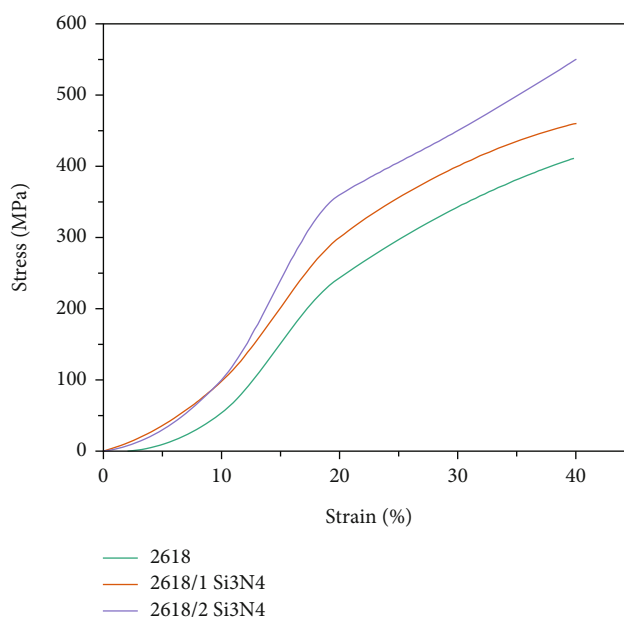


FIGURE 3: Curves of the samples' compression stress and strain.

conduct precise measurements using the metallographic preparation. A 1 kg load and a dwell time of 20 seconds were used to measure hardness. The average of five successful indentations was calculated. A universal testing machine with a 0.5 mm/min test speed was used for the compression tests. A pin-on-disc test device was used to conduct wear tests under dry sliding conditions. Temperatures ranging from 50 to 250 degrees Celsius were used for wear tests at a sliding speed of 120 millimetres per second with loads of 15 to 45 Newtons. The sliding distance was 200 metres. The AISI 52100 steel used for the counterface had a hardness rating of 63 HRC. Figure 2 shows pin on disc wear setup.

2.3. The Experiment Design. The Taguchi method was used with three factors and three levels. Si₃N₄ content, load, and temperature were all factors in the experiment. Table 1 provides the values of the parameters. The Taguchi design used the L27 array.

3. Results and Discussion

Table 2 displays the specimens' densities and hardness of the produced composites.

TABLE 3: Fabricated samples' mechanical properties.

Materials	Grain size,	CYS, Mpa	UCS
AA 2618	20.2	276.2 ± 11.2	516.7 ± 14.2
AA 2618/1% silicon nitrate	19.4	302.6 ± 10.2	591.6 ± 23.4
AA 2618/2% silicon nitrate	15.6	324.6 ± 9.1	665.8 ± 20.1

3.1. Mechanical Properties. According to these results, increasing the amount of Si₃N₄ results in greater compressive yield strength (CYS) and ultimate compressive strength (UCS). Comparing the CYS and UCS of the AA 2618/2Si₃N₄ composite to those of the AA 2618 alloy, 17.2% and 28.9% increases were observed. Figure 3 shows the curves of the samples compression stress and strain. Table 3 summarises the mechanical properties and average grain size for each type of cereal grain. The dislocations are also slowed by the presence of reinforcing particles. Due to the occurrence of reinforcement elements and an increased grain boundary area as a result of grain refinement, dislocation movement

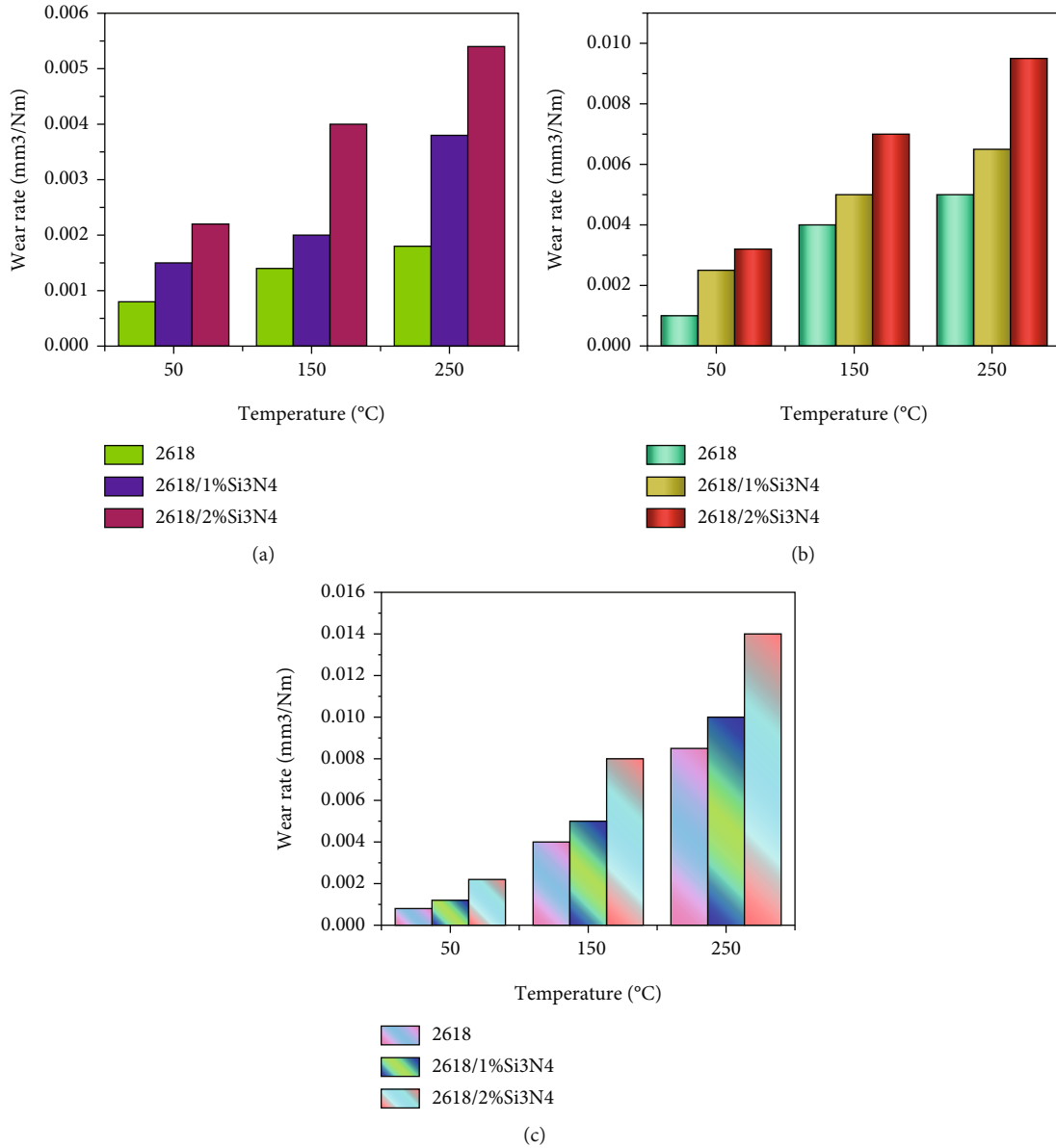


FIGURE 4: Temperature affects the rate of wear on the load: (a) 50°C, (b) 150°C, and (c) 250°C.

is hindered. As a result, the strongest material has the smallest grain size. Grain size decreases as the Si₃N₄ content increases. AA 2618/1Si₃N₄ and AA 2618/2Si₃N₄ reduced the grain size by 7.8 percent and 21.9 percent, respectively, when compared to the AA 2618 alloy. Sintering grain refinement may be attributed to the hard Si₃N₄ elements in the structure acting as a wall to grain limit movement. There is also evidence to suggest that nano-reinforcement slows down grain growth by causing pinning at grain boundaries. It is also crucial to have a mechanism for transferring the weight of the load. The transmission of loads from the soft matrix to hard fortification particles has been credited with increasing the strength of composite materials. The interfacial bonding between the matrix material and the reinforcement particles is responsible for the increased strength.

Using Si₃N₄ particles, the researchers were able to transfer loads from a matrix to a reinforcement. Al matrix composites reinforced with nanoparticles can also benefit from the Orowan strengthening mechanism. Nanoparticles are used to form residual dislocation loops in the Orowan strengthening mechanism. The back stress created by the dislocation loops prevents the dislocation from moving forward. Composite materials become stronger as a result.

3.2. Wear Results

3.2.1. The Effect of Load on the Rate of Wear. There was a clear correlation between increasing load and increasing wear rate at all temperatures. Aside from that, the AA 2618/2Si₃N₄ composite's wear rate was the lowest. The

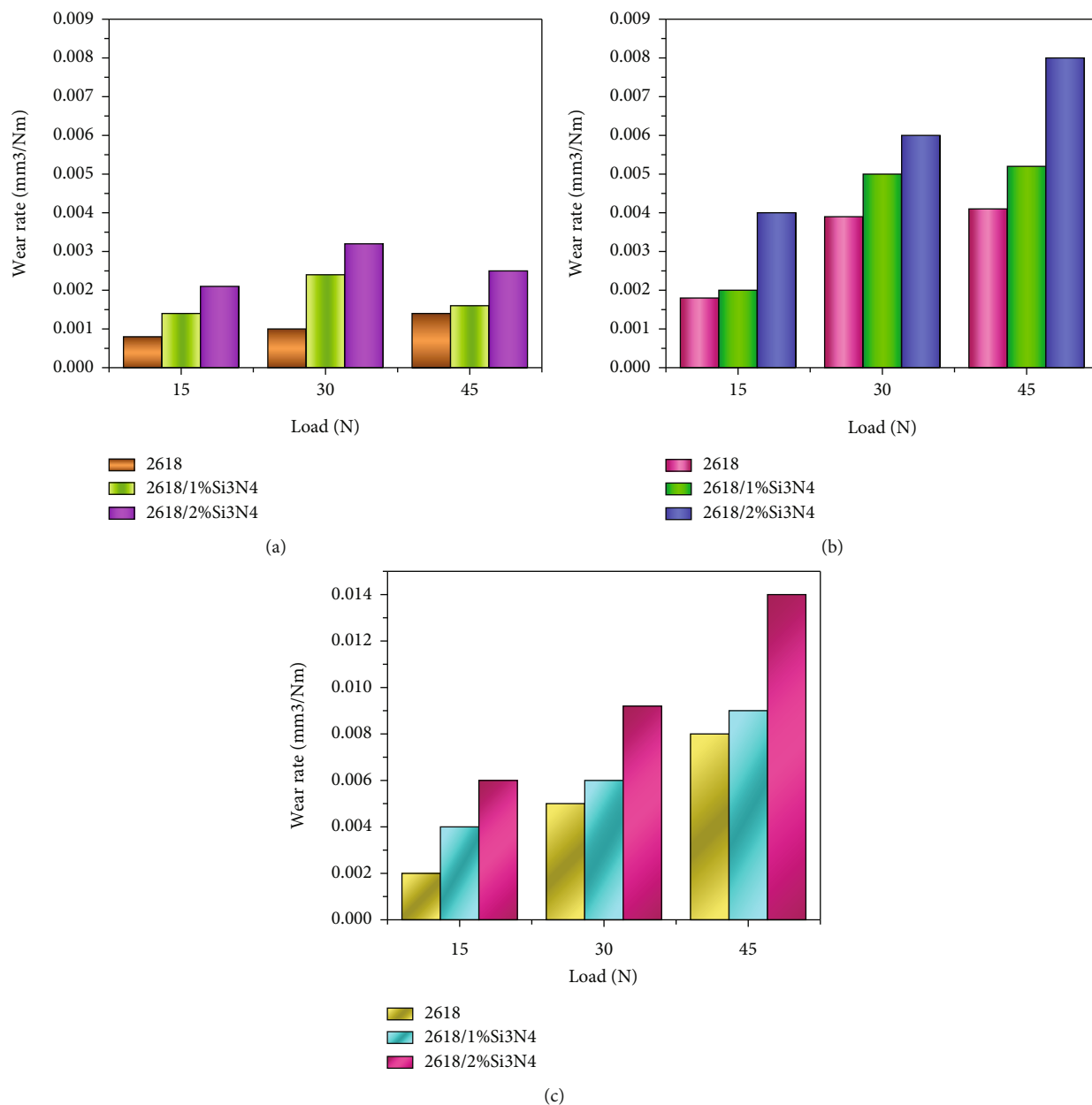


FIGURE 5: Temperature-dependent wear rates under a variety of load conditions: (a) 15 N, (b) 30 N, and (c) 45 N.

lubricating effect of Si₃N₄ particles contributes to the improved wear resistance of composites. Due to the Si₃N₄ particles, composite materials have a lower rate of wear because the metallic contact between sliding surfaces is reduced. A 45 N load on AA 2618/2Si₃N₄ reduces wear rates by 45.8 percent, 42.1 percent, and 35.7 percent compared to an unreinforced alloy at 50°C, 150°C, and 250°C. As the temperature rises, the wear rates of the samples also increase significantly. At temperatures of 50°C, 150°C, and 250°C, AA 2618 has a wear rate of 0.0024 mm⁻³/Nm. for the alloy, according to research.

Dislocation density increases when there is a mismatch in thermal expansion. This has a significant impact on the hardness of composite materials. Grains of AA 2618/Si₃N₄

composites have fewer grain boundaries, resulting in a higher wear resistance. The dislocation movement is hindered by the increased grain boundaries. The improvement in tribological performance was attributed to this. The improved wear performance of AA 2618/Si₃N₄ composites is due to the increased hardness and mechanical properties of the strengthening mechanisms.

3.2.2. Temperature Effect on Wear Rate. With increasing Si₃N₄ content at temperatures between 50 and 250 degrees Celsius, the wear rate of AA 2618/Si₃N₄ composites is reduced. Al matrix thermal stability is said to improve as the amount of Si₃N₄ in the alloy increases. The wear rate of the models also increases the temperature of the test

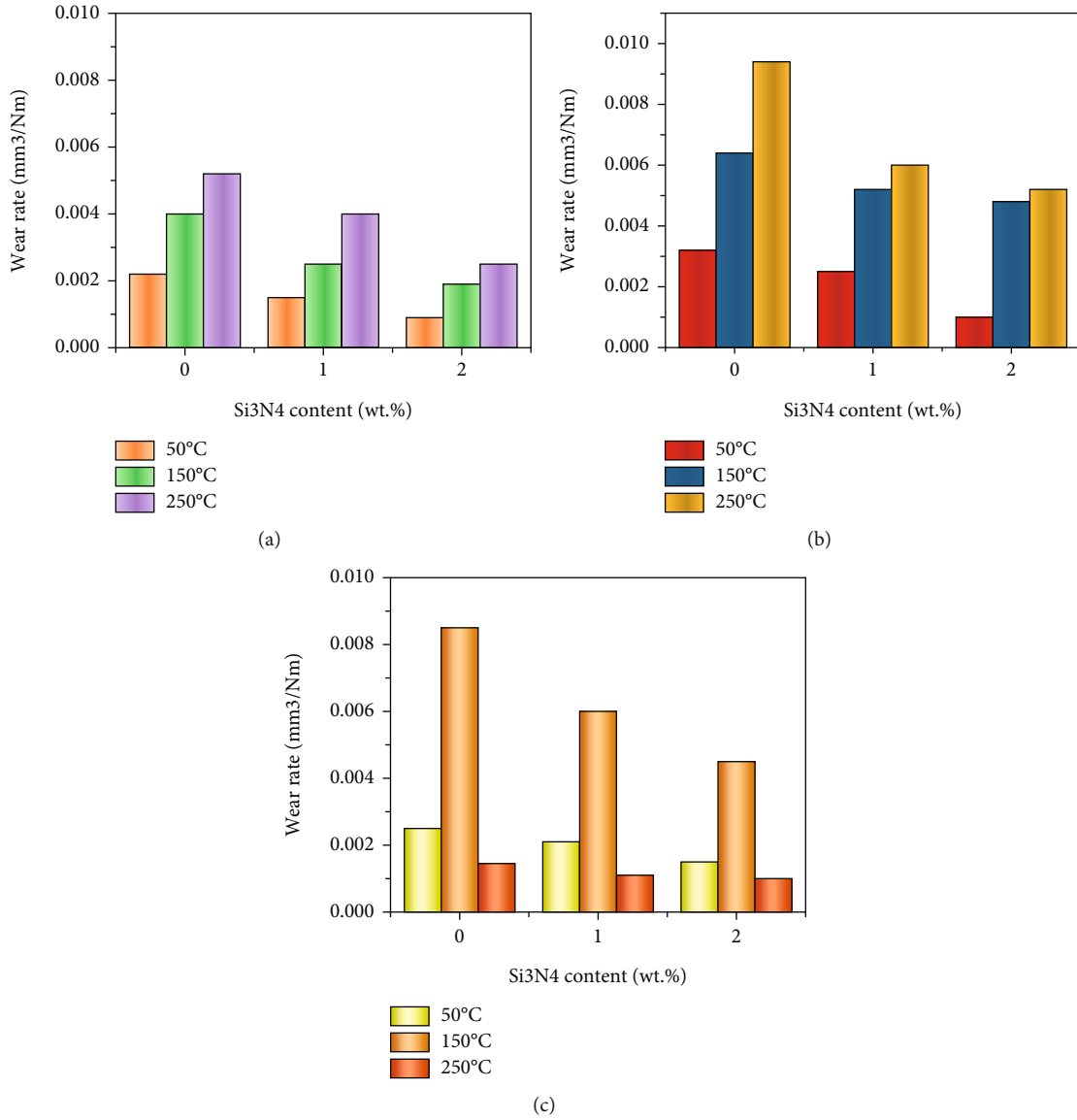


FIGURE 6: Si₃N₄ content's wear rate under various loads: (a) 15 N, (b) 30 N, and (c) 45 N.

increases. As the test temperature rises, the softening trend becomes more pronounced.

3.2.3. Effect of Wear Rate on Silicon Nitride. AA 2618 alloy wear rate is thought to be affected by silicon nitride content below 15 N, 30 N, and 45 N loads at temperatures of 50°C, 150°C, and 250°C. After adding Si₃N₄, the wear performance was noticeably improved in all conditions. Sample and counterface material are subjected to low shear stress because of Si₃N₄ particles in the structure. At a temperature of 250°C and a load of 45 N, the AA 2618 alloy showed severe wear.

3.2.4. Coefficient of Friction. In this graph, friction coefficient (COF) is plotted against load and temperature. Under all wear conditions, it can be seen that friction

coefficient reduces with increasing silicon nitride content. The COF of the samples rises in direct proportion to the increase in load and test temperature. The AA 2618/2Si₃N₄ sample had the lowest COF. This resulted in an average COF value of 0.333 for AA 2618/1Si₃N₄ and 0.210 for the AA 2618/2Si₃N₄ samples tested at a temperature of 50°C. At a temperature of 250 degrees Celsius and a load of 45 Newton, the average COF values of AA 2618/1Si₃N₄ were 0.668, 0.572, and 0.474, respectively, and all are shown in Figures 4 and Figure 5. Composites have low coefficients of friction because of a solid lubricant, Si₃N₄. Furthermore, it was discovered that the presence of hard reinforcement particles reduces the actual contact area between the counterface and the matrix. As a result, composite materials have a lower COF. It is well established that the matrix softens as the temperature rises.

TABLE 4: Taguchi L_{27} orthogonal array results and response value values.

Ex.No	Load	Temp	Si_3N_4 wt%	Wear rate	Ratio of S/N
1	15	50	0	0.0028	54665
2	15	50	1	0.0016	570881
3	15	50	2	0.0009	628482
4	15	150	0	0.0042	492846
5	15	150	1	0.0023	541128
6	15	150	2	0.0018	561086
7	15	250	0	0.0059	462127
8	15	250	1	0.0041	491218
9	15	250	2	0.0026	551342
10	30	50	0	0.0038	489720
11	30	50	1	0.0029	521535
12	30	50	2	0.0019	610012
13	30	150	0	0.0071	450182
14	30	150	1	0.0056	466710
15	30	150	2	0.0049	481312
16	30	250	0	0.0099	413421
17	30	250	1	0.0069	452817
18	30	250	2	0.0059	470816
19	45	50	0	0.0031	530124
20	45	50	1	0.0024	558428
21	45	50	2	0.0024	581868
22	45	150	0	0.0091	421868
23	45	150	1	0.0069	461828
24	45	150	2	0.0054	472858
25	45	250	0	0.0152	381824
26	45	250	1	0.0112	391524
27	45	250	2	0.0096	411015

As the counterface and matrix become more adherent, so does the matrix's adhesion to the counterface material. As a result, the samples' COF rises.

Adding Si_3N_4 particles improves wear performance in this study, according to researchers. The COF is also found to be reduced when Si_3N_4 particles are added. The wear behaviour of Si_3N_4 -reinforced aluminium composites was identified to be similar by several researchers. The Al matrix's wear performance was reported to have improved, and the COF was reported to have decreased and it is shown in Figure 6. Composites with the addition of Si_3N_4 reinforcement were found to be more resistant to wear because of the material's lubricant properties. Due to the matrix strengthening that occurred as dislocation density increased, wear resistance also increased.

Grain refinement and particle dispersion strengthening were both associated with an increase in composite strength and hardness. Composites have grain sizes that are smaller than those of the AA 2618 alloy, as shown in Table 3. Counterface material and matrix are separated by a thin layer of oxide, according to this theory. In this study, the surface was found to be oxidised when heated to high temperatures.

4. Statistical Analysis

4.1. ANOVA Results. Table 4 displays the Taguchi L_{27} orthogonal array results and response value values. The experimental data was analysed using ANOVA. ANOVA can be used to find which variables have greatest impact on the rate at which clothing wears out. The ANOVA studies were conducted with a 95% level of confidence. The ANOVA results are shown in Table 5. Temperature is widely believed to be the most significant factor in the rate of wear (46.21 percent). Load and Si_3N_4 content were found to be responsible for 23.97 percent and 12.92 percent of the total. Interactions appear to have a smaller impact than individual parameters. There is a 13.67 percent correlation between load and temperature, followed by a correlation between temperature and Si_3N_4 (2.43 percent).

Temperature and Si_3N_4 content were independent variables. It was determined that the wear rate was the dependent variable. The wear rate of samples was predicted using a linear and a nonlinear regression model and it is shown in Figures 7 and 8.

TABLE 5: The results of the ANOVA test for each sample.

Source	Degrees of freedom	Seq SS	% of contribution	Adj SS	Adj MS	F value	P value
Load (L)	2	0.000071	23.4	0.000071	0.000038	168.94	0.0000
Temperature (°C)	2	0.000138	46.4	0.000134	0.000069	316.18	0.0000
Si ₃ N ₄ wt%	2	0.000039	11.69	0.000039	0.000021	89.14	0.0000
L x T	4	0.000002	14.24	0.000041	0.000015	17.86	0.0000
L x Si ₃ N ₄	4	0.000009	0.31	0.000001	0.0000	0.79	0.5960
T x Si ₃ N ₄	4	0.000003	3.35	0.000008	0.00003	8.96	0.00070
Error	8	0.000289	0.61	0.000003	0.00000		
Total	26		100				

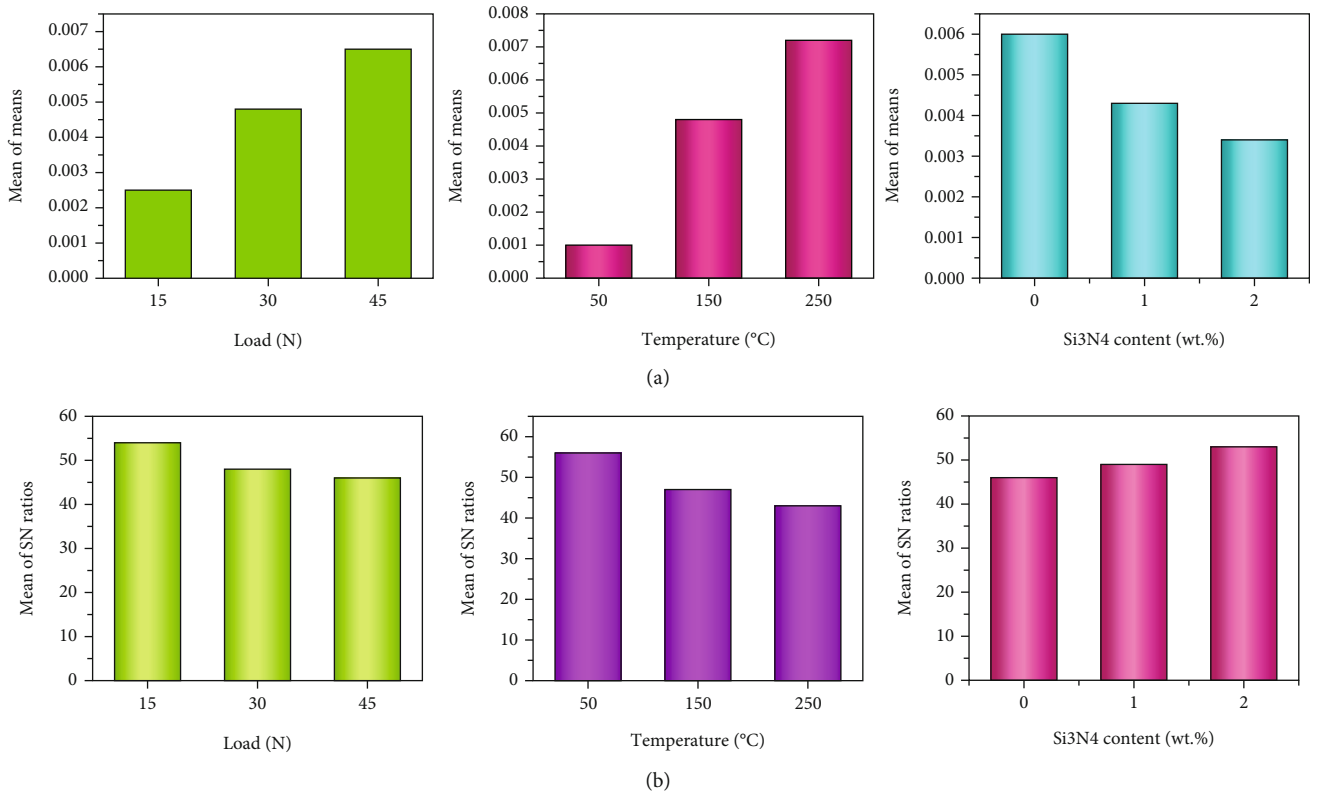


FIGURE 7: (a) Wear rate and (b) S/N ratios for the samples are shown in the main effects plots.

4.2. Analysis of S/N Ratios. This research made use of 27-row, 3-column full-factorial arrays. The constraints, wear rate, and signal-to-noise ratio are listed. Using the S/N ratio “Small is better” characteristic, this study was able to determine the wear rate. Each variable’s impact on output was evaluated using the S/N ratio. Given here is the S/N Ratio (S/N) in equation (1)

$$S/N = -10 \log \frac{1}{n} \left(\sum_{i=1}^n y_i^2 \right). \quad (1)$$

Signal-to-noise ratio (S/N) is the ratio of a signal’s strength to the background noise, and n is how many trials were conducted. This study looked at how different loads,

temperatures, and levels of Si₃N₄ content affected wear rates. Table 6 summarises the relative importance of various wear test parameters and their respective means. The best results are achieved when the S/N ratio of the combination of wear rate-related parameters is the highest. There is a correlation between wear rate and temperature, which is more pronounced than the effects of load and Si₃N₄. The effect of Si₃N₄ content was overshadowed by the effect of load. Plots’ wear rates are the primary goal of the analysis. Alloy AA 2618 must have a low wear rate and high Si₃N₄ content in order to function properly. For the interaction plots, the non-parallelism effect is well-known. If the interaction plot’s lines are not parallel, a finding of low interaction is valid. The wear parameters interact strongly at the intersection of lines. The relationship between load and temperature can

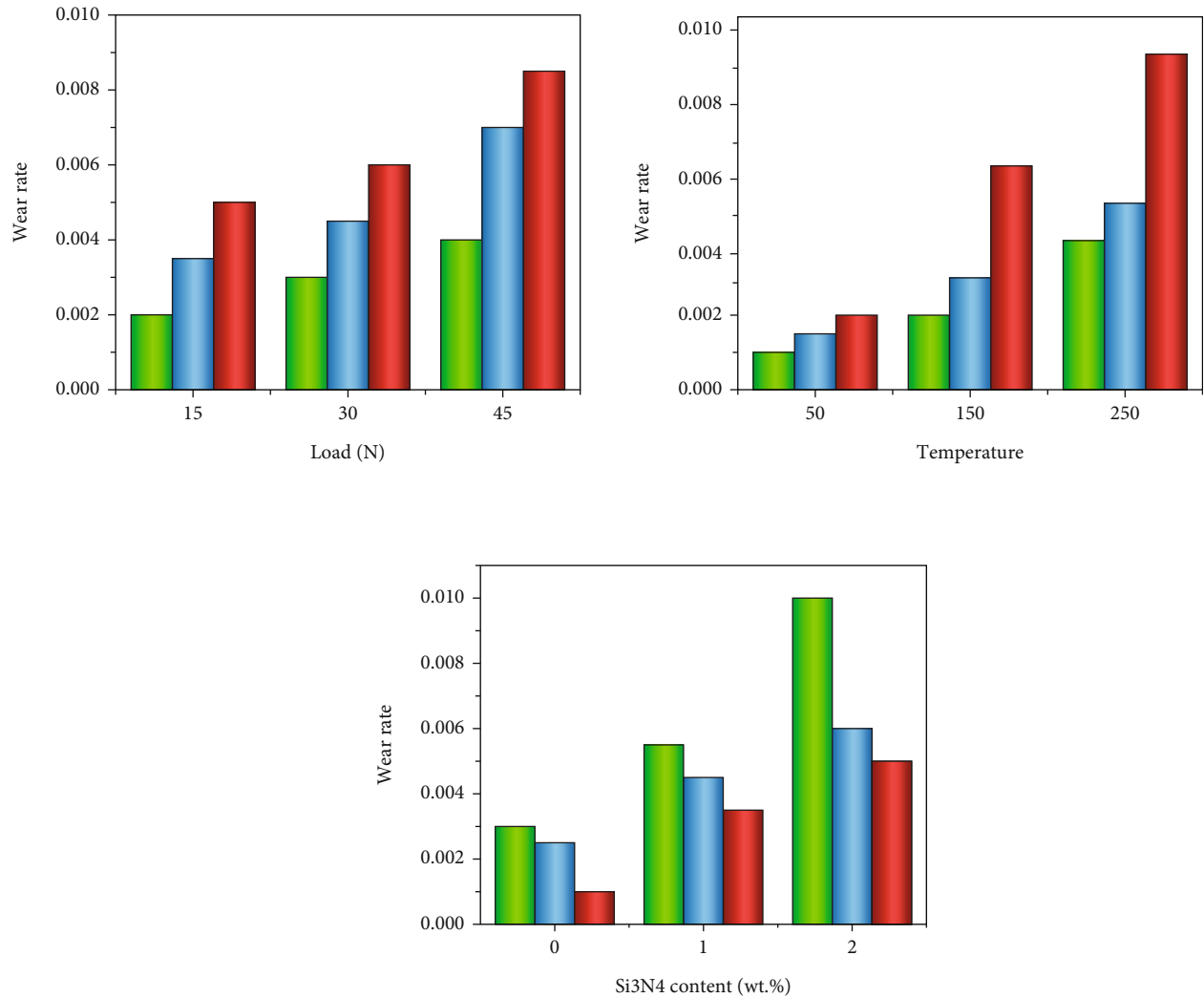


FIGURE 8: Wear rate is plotted as a function of the interaction between wear parameters.

TABLE 6: Responses to the sample S/N ratios.

Levels	Applied load	Temperature of control factors °C	Wt% of Si ₃ N ₄ content
1	54.8	54.8	46.4
2	48.6	48.4	49.8
3	47.1	45.2	53.3
Delta	8.1	13.1	7.4
Rank	2	1	3

be clearly seen. Temperature Si₃N₄ content and load Si₃N₄ content had a low interaction. The signal-to-noise ratio compares the strength of a signal to the background noise.

4.3. Evaluation Parameters. Regression models were assessed against two criteria in this study. R^2 and root mean square error were used to calculate the determination coefficient,

R^2 (RMSE). The following equations were used to calculate the RMSE in equation (2) and R^2 in equation (3).

$$\text{RMSE} = 1 - \left(\frac{1}{n} \sum_{i=1}^n (e_i - p_i)^2 \right)^{1/2}. \quad (2)$$

There are two values: e_i is the actual and p_i is the predicted one, respectively.

$$R^2 = 1 - \left(\frac{\sum_{i=1}^n (e_i - p_i)^2}{\sum_{i=1}^n (e_i - \bar{p}_i)^2} \right)^{1/2}. \quad (3)$$

For the regression models, R^2 is a measure of how well they perform based on the mean of the actual values. High R^2 and low RMSE values are what we are looking for in the model we are building here. Linear and nonlinear regressions have RMSE values of 0.0013 and 0.0009, respectively, for the two methods as in Figures 7 and 8. For linear and nonlinear

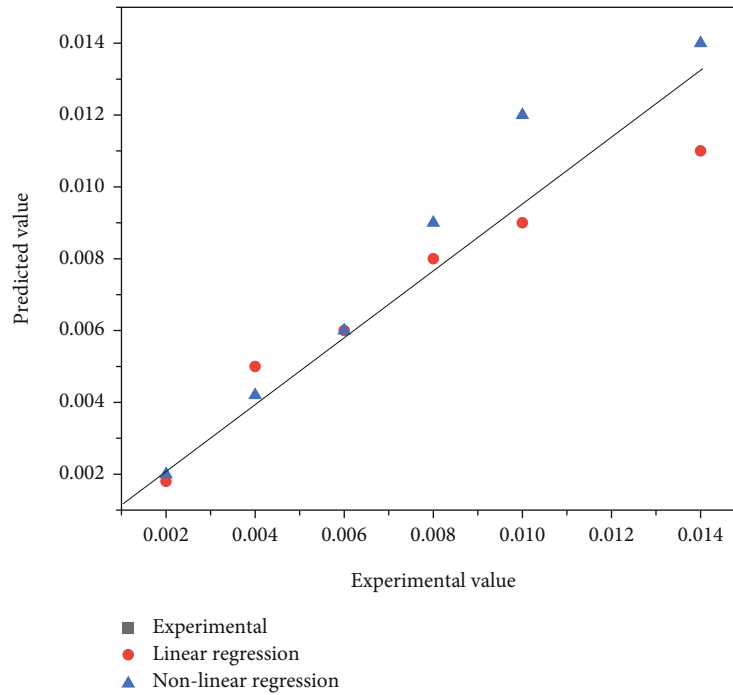


FIGURE 9: The dataset's regression model results.

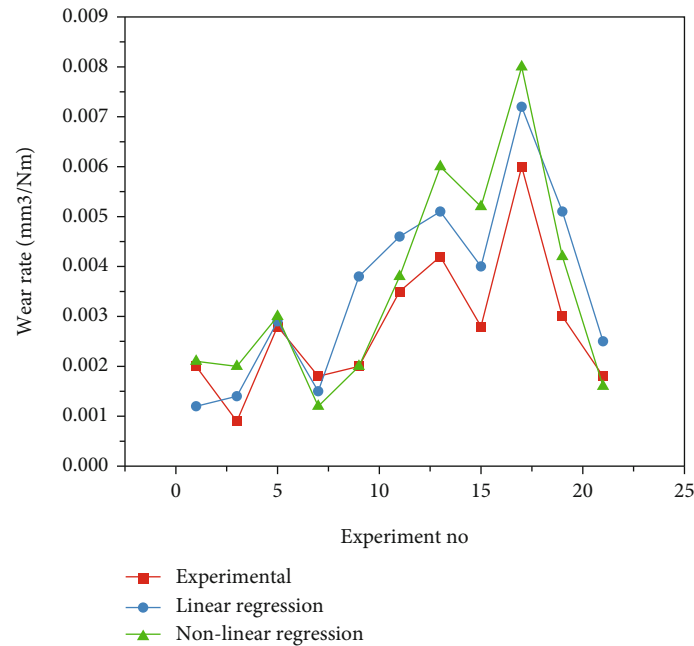


FIGURE 10: Comparison of experiment and predicted values.

regressions, the R^2 (percent) was 84.8 and 91.5, respectively. Regression models with low RMSE values are more likely to be successful. Nonlinear regression models outperformed linear regression models by 1.4 times as in tables.

Prediction accuracy is higher in models that use nonlinear regression than in linear regression models. Lower prediction values were obtained by using a linear regression model. For AA 2618/Si₃N₄ composites, nonlinear regression can be used to accurately predict the wear rate. Tribological

studies can save money and time by using the nonlinear regression model as shown in Figures 9 and 10.

5. Conclusions

This work used experimental and statistical approaches to investigate the wear behaviour of AA 2618/Si₃N₄ (1 and 2wt percent) composites. The following findings were obtained from this investigation. In all test settings, composites

containing AA 2618/2 wt percent Si₃N₄ demonstrated the best wear resistance. Delamination was most noticeable at 50 degrees Celsius, with substantial delamination and metal flow occurring at 250 degrees Celsius.

- (i) There was a 47.32 percent temperature, 24.96 percent load, and 12.51 percent Si₃N₄ content contribution to wear rate, respectively
- (ii) Linear regression had an R^2 of 83.4%, while nonlinear regression had an R^2 of 92.8%. By using nonlinear regression to predict wear rate, examining time and the number of examinations can be reduced
- (iii) Because of their superior elevated temperature tribological performance, AA 2618 with Si₃N₄ composites are the best choice for wear applications at high temperatures

Data Availability

The data used to support the findings of this study are included within the article. Further data or information is available from the corresponding author upon request.

Conflicts of Interest

The authors declare that there are no conflicts of interest regarding the publication of this paper.

Acknowledgments

The authors appreciate the supports from Wolaita Sodo University, Ethiopia, for the research and preparation of the manuscript. The authors thank the RMK Engineering College, and Aditya Engineering College for providing assistance to this work. Taif University Researchers Supporting Project number (TURSP-2020/01), Taif University, Taif, Saudi Arabia.

References

- [1] E. Georgantzia, M. Gkantou, and G. S. Kamaris, "Aluminium alloys as structural material: a review of research," *Engineering Structures*, vol. 227, article 111372, 2021.
- [2] K. Subramani, T. Arunkumar, V. Mohanavel et al., "Investigation on wear characteristics of Al 2219/Si₃N₄/Coal bottom ash MMC," *Materials Today: Proceedings*, vol. 62, no. 8, pp. 5514–5518, 2022.
- [3] M. A. Afifah, O. M. Zaidi, H. Hanizam, S. M. Shukor, and M. I. Fadhilina, "Recent development in graphene-reinforced aluminium matrix composite: a review," *Reviews on Advanced Materials Science*, vol. 60, no. 1, pp. 801–817, 2021.
- [4] P. Ashwath, J. Joel, M. A. Xavier, and H. P. Kumar, "Effect of SiC and Al₂O₃ particles addition to AA 2900 and AA 2024 MMC's synthesized through microwave sintering," *Mater. Today-Proc.*, vol. 5, no. 2, pp. 7329–7336, 2018.
- [5] M. I. Ul Haq and A. Anand, "Dry sliding friction and wear behavior of AA7075-Si₃N₄ composite," *Silicon*, vol. 10, no. 5, pp. 1819–1829, 2018.
- [6] L. Zhang, Z. Wang, Q. Li et al., "Microtopography and mechanical properties of vacuum hot pressing Al/B₄C composites," *Ceramics International*, vol. 44, no. 3, pp. 3048–3055, 2018.
- [7] M. Irfan Ul Haq, A. Raina, A. Anand, S. M. Sharma, and R. Kumar, "Elucidating the effect of MoS₂ on the mechanical and tribological behavior of AA7075/Si₃N₄ composite," *Journal of Materials Engineering and Performance*, vol. 29, no. 11, pp. 7445–7455, 2020.
- [8] V. Mohanavel and M. Ravichandran, "Influence of AlN particles on microstructure, mechanical and tribological behaviour in AA6351 aluminum alloy," *Materials Research Express*, vol. 6, no. 10, article 106557, 2019.
- [9] M. L. Bharathi, S. Adarsh Rag, L. Chitra et al., "Investigation on wear characteristics of AZ91D/nanoalumina composites," *Journal of Nanomaterials*, vol. 2022, Article ID 2158516, 9 pages, 2022.
- [10] M. N. Akhtar, T. Sathish, V. Mohanavel et al., "Optimization of process parameters in CNC turning of aluminum 7075 alloy using L27 array-based Taguchi method," *Materials*, vol. 14, no. 16, p. 4470, 2021.
- [11] M. R. Akbarpour and A. Pouresmaeil, "The influence of CNTs on the microstructure and strength of Al-CNT composites produced by flake powder metallurgy and hot pressing method," *Diamond and Related Materials*, vol. 88, pp. 6–11, 2018.
- [12] E. Ghasali, P. Sangpour, A. Jam, H. Rajaei, K. Shirvanimoghaddam, and T. Ebadzadeh, "Microwave and spark plasma sintering of carbon nanotube and graphene reinforced aluminum matrix composite," *Arch. Civ. Mech. Eng.*, vol. 18, no. 4, pp. 1042–1054, 2018.
- [13] M. E. Turan and F. Aydin, "Improved elevated temperature mechanical properties of graphene-reinforced pure aluminium matrix composites," *Materials Science and Technology*, vol. 36, no. 10, pp. 1092–1103, 2020.
- [14] X. Zeng, J. Teng, J. G. Yu, A. S. Tan, D. F. Fu, and H. Zhang, "Fabrication of homogeneously dispersed graphene/Al composites by solution mixing and powder metallurgy," *Int. J. Min. Met. Mater.*, vol. 25, no. 1, pp. 102–109, 2018.
- [15] J. Su and J. Teng, "Recent Progress in graphene-reinforced aluminum matrix composites," *Frontiers of Materials Science*, vol. 15, no. 1, pp. 79–97, 2021.
- [16] X. Zeng, J. Yu, D. Fu, H. Zhang, and J. Teng, "Wear characteristics of hybrid aluminum-matrix composites reinforced with well-dispersed reduced graphene oxide nanosheets and silicon carbide particulates," *Vacuum*, vol. 155, pp. 364–375, 2018.
- [17] S. K. Selvaraj, M. K. Nagarajan, and L. A. Kumaraswamidhas, "An investigation of abrasive and erosion behaviour of AA 2618 reinforced with Si₃N₄, AlN and ZrB₂ in situ composites by using optimization techniques," *Archiv.Civ.Mech.Eng.*, vol. 17, no. 1, pp. 43–54, 2017.
- [18] K. B. Lee, H. S. Sim, S. W. Heo, H. R. Yoo, S. Y. Cho, and H. Kwon, "Tensile properties and microstructures of Al composite reinforced with BN particles," *Composites. Part A, Applied Science and Manufacturing*, vol. 33, no. 5, pp. 709–715, 2002.
- [19] S. Sardar, S. K. Karmakar, and D. Das, "High stress abrasive wear characteristics of Al 7075 alloy and 7075/Al₂O₃ composite," *Measurement*, vol. 127, pp. 42–62, 2018.
- [20] J. M. Mistry and P. P. Gohil, "Experimental investigations on wear and friction behaviour of Si₃N₄P reinforced heat-

- treated aluminium matrix composites produced using electromagnetic stir casting process,” *Compos. Part. B-Eng.*, vol. 161, pp. 190–204, 2019.
- [21] N. Idusuyi and J. I. Olayinka, “Dry sliding wear characteristics of aluminium metal matrix composites: a brief overview,” *Journal of Materials Research and Technology*, vol. 8, no. 3, pp. 3338–3346, 2019.
- [22] N. Kaushik and S. Singhal, “Wear conduct of aluminum matrix composites: a parametric strategy using Taguchi based GRA integrated with weight method,” *Cogent. Eng.*, vol. 5, no. 1, p. 1467196, 2018.
- [23] A. H. Idrisi and A. H. I. Mourad, “Wear performance analysis of aluminum matrix composites and optimization of process parameters using statistical techniques,” *Metallurgical and Materials Transactions A: Physical Metallurgy and Materials Science*, vol. 50, no. 11, pp. 5395–5409, 2019.
- [24] M. O. Bodunrin, K. K. Alaneme, and L. H. Chown, “Aluminium matrix hybrid composites: a review of reinforcement philosophies; mechanical, corrosion and tribological characteristics,” *Journal of Materials Research and Technology*, vol. 4, no. 4, pp. 434–445, 2015.
- [25] R. A. Khatavkar, A. K. Mandave, D. D. Baviskar, and S. L. Shinde, “Influence of hexagonal boron nitride on tribological properties of AA 2618-HSI3N4 metal matrix composite,” *Int. Res. J. Eng. Technol.*, vol. 5, no. 5, pp. 3792–3798, 2018.
- [26] T. Gangatharan, A. A. Moorthy, and T. Rameshkumar, “Enhancing the tribological properties of composite materials for centrifugal pump applications,” *IRJET*, vol. 3, no. 3, pp. 195–199, 2016.
- [27] H. Chi, L. Jiang, G. Chen, P. Kang, X. Lin, and G. Wu, “Dry sliding friction and wear behavior of (TiB₂ + h-BN)/2024Al composites,” *Materials and Design*, vol. 87, pp. 960–968, 2015.
- [28] P. Paulraj and R. Harichandran, “The tribological behavior of hybrid aluminum alloy nanocomposites at high temperature: role of nanoparticles,” *Journal of Materials Research and Technology*, vol. 9, no. 5, pp. 11517–11530, 2020.
- [29] M. M. Boopathi, K. P. Arulshri, and N. Iyandurai, “Evaluation of mechanical properties of aluminium alloy 2024 reinforced with silicon carbide and fly ash hybrid metal matrix composites,” *American Journal of Applied Sciences*, vol. 10, no. 3, pp. 219–229, 2013.
- [30] M. E. Turan, Y. Sun, F. Aydin, H. Zengin, Y. Turen, and H. Ahlatci, “Effects of carbonaceous reinforcements on microstructure and corrosion properties of magnesium matrix composites,” *Materials Chemistry and Physics*, vol. 218, pp. 182–188, 2018.
- [31] F. Aydin and M. E. Turan, “The effect of boron nitride on tribological behavior of mg matrix composite at room and elevated temperatures,” *Journal of Tribology*, vol. 142, no. 1, pp. 1–7, 2020.
- [32] M. Rahimian, N. Parvin, and N. Ehsani, “The effect of production parameters on microstructure and wear resistance of powder metallurgy Al-Al₂O₃ composite,” *Materials and Design*, vol. 32, no. 2, pp. 1031–1038, 2011.
- [33] F. Aydin and Y. Sun, “Investigation of wear behaviour and microstructure of hot-pressed TiB₂ particulate-reinforced magnesium matrix composites,” *Canadian Metallurgical Quarterly*, vol. 57, no. 4, pp. 455–469, 2018.
- [34] R. Prasad, H. Kumar, P. Kumar, S. P. Tewari, and J. K. Singh, “Microstructural, mechanical and tribological characterization of friction stir welded A7075/ZrB₂ in situ composites,” *Journal of Materials Engineering and Performance*, vol. 30, no. 6, pp. 4194–4205, 2021.